International Journal of Nanomedicine

Dovepress
open access to scientific and medical research

Open Access Full Text Article

ORIGINAL RESEARCH

Codelivery of SH-aspirin and curcumin by mPEG-PLGA nanoparticles enhanced antitumor activity by inducing mitochondrial apoptosis

This article was published in the following Dove Press journal:
International Journal of Nanomedicine
18 August 2015
Number of times this article has been viewed

Lin Zhou[1,2,*]
Xingmei Duan[1,2,*]
Shi Zeng[1]
Ke Men[1]
Xueyan Zhang[1]
Li Yang[1]
Xiang Li[1]

[1]State Key Laboratory of Biotherapy, Cancer Center and Department of Urology, West China Hospital, Sichuan University, Chengdu, People's Republic of China; [2]Sichuan Food and Drug Safety Monitoring and Review of Certification, Adverse Reaction Monitoring Center, Drug Abuse Monitoring Center, Chengdu, People's Republic of China

*These authors contributed equally to this work

Abstract: Natural product curcumin (Cur) and H_2S-releasing prodrug SH-aspirin (SH-ASA) are potential anticancer agents with diverse mechanisms, but their clinical application prospects are restricted by hydrophobicity and limited efficiency. In this work, we coencapsulated SH-ASA and Cur into methoxy poly(ethylene glycol)-poly (lactide-coglycolide) (mPEG-PLGA) nanoparticles through a modified oil-in-water single-emulsion solvent evaporation process. The prepared SH-ASA/Cur-coloaded mPEG-PLGA nanoparticles had a mean particle size of 122.3±6.8 nm and were monodispersed (polydispersity index =0.179±0.016) in water, with high drug-loading capacity and stability. Intriguingly, by treating with SH-ASA/Cur-coloaded mPEG-PLGA nanoparticles, obvious synergistic anticancer effects on ES-2 and SKOV3 human ovarian carcinoma cells were observed in vitro, and activation of the mitochondrial apoptosis pathway was indicated. Our results demonstrated that SH-ASA/Cur-coloaded mPEG-PLGA nanoparticles could have potential clinical advantages for the treatment of ovarian cancer.

Keywords: drug delivery, cancer therapy, ovarian cancer, synergistic effect

Introduction

Cancer is the leading cause of death in economically developed countries and the second leading cause of death in developing countries.[1] Ovarian cancer is the most frequently diagnosed cancer in females, with nearly 225,900 cases and 140,200 deaths estimated in 2008 worldwide.[1] Recent research has indicated that ovarian cancer is a general term for a series of molecularly and etiologically distinct diseases that simply share an anatomical location.[2] As a result, therapeutic agents with high efficiency are in great need.

Medicines derived from plants play an important role in cancer therapy. Curcumin (Cur) (diferuloylmethane, a polyphenol) is an active principle of the perennial herb *Curcuma longa* (commonly known as turmeric); its molecular structure is presented in Figure 1A. Several studies have reported the therapeutic effects of Cur including anticancer activity.[3–6] It has been indicated that Cur is able to suppress several types of cancers, including human breast cancer, colon cancer, and head and neck squamous cell carcinoma.[7–16] Until now, many studies have been performed to uncover its multiple cellular targets and molecular mechanisms.[17–20] Molecular targets in cancer treatment by Cur were gradually revealed, including transcription factors, growth factors, kinases, inflammatory cytokines, adhesion molecules, and apoptosis-related proteins.[21] Besides, it has been reported that Cur has potential in overcoming multidrug resistance.[22] It has also demonstrated synergistic antitumor effects with some other anticancer agents.[23–26] Besides, a Phase IIa clinical trial of Cur for the prevention of colorectal neoplasia has

Correspondence: Li Yang
State Key Laboratory of Biotherapy and Cancer Center, West China Hospital, West China Medical School, Sichuan University, Chengdu 610041, People's Republic of China
Tel +86 028 8516 4061
Fax +86 028 8516 4060
Email yl.tracy73@gmail.com

Xiang Li
State Key Laboratory of Biotherapy and Department of Urology, West China Hospital, Sichuan University Chengdu, 610041, People's Republic of China
Tel +86 028 851 640 61
Fax +86 028 8516 4060
Email xiangli.87@163.com

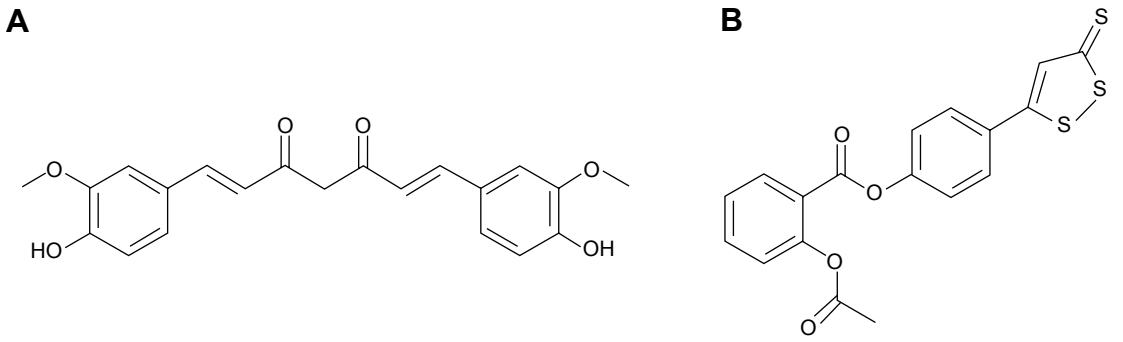

Figure 1 Molecular structures of curcumin and SH-aspirin.
Notes: (**A**) Curcumin; (**B**) SH-aspirin.

showed good results.[27] Although the therapeutic activities of Cur demonstrate its potential in cancer therapy, the issue of water insolubility greatly limits its further application, such as in drug formulation.

Hydrogen sulfide (H_2S) plays a fundamental role in the regulation of a variety of cellular and physiological functions at appropriate concentrations. As an important endogenous modulator, it has beneficial effects as an anti-inflammatory and antiperoxidative agent in inflammation, oxidative stress, and angiogenesis.[28] Several H_2S-releasing drugs (or prodrugs) have been developed to conjugate the beneficial effects of H_2S with those of other pharmaceuticals.[29] SH-aspirin (SH-ASA) is one of these H_2S-releasing nonsteroidal anti-inflammatory drugs (HS-NSAIDs), in which the H_2S-releasing moiety is covalently attached to aspirin (Figure 1B). Its H_2S-releasing ability was realized through the hydrolysis of the ester bond in SH-ASA. In recent years, SH-ASA has showed strong inhibitory effects on the growth properties of different cancer cells, including human colon, breast, pancreatic, and prostate cancers.[30–32] However, SH-NSAIDs, including SH-ASA, have several drawbacks that limit their development as pharmaceuticals. For example, they usually have relatively high half maximal inhibitory concentrations (IC_{50}s) and difficulties with water solubility.[33]

Nanotechnology provides a novel method to overcome the solubility issue of hydrophobic drugs.[34] Encapsulation of those drugs in nanoparticles can render them completely dispersible in aqueous solutions. Moreover, drug-loaded nanoparticles demonstrated prolonged drug release behavior and high stability.[35] Polymer-based nanocarriers are considered to be excellent candidates for anticancer drug-delivery systems, and some biodegradable polymer nanoparticle-delivered anticancer drugs have already been marketed.[36] The methoxy poly(ethylene glycol)-poly (lactide-coglycolide) (mPEG-PLGA) copolymer is biodegradable, amphiphilic, and easy to produce, showing promising application in drug-delivery systems. Recently, there have been several reports about the use of mPEG-PLGA nanoparticles for anticancer agent delivery and cell-scaffold development.[37–39] Thus, in this study, we attempted to develop an SH-ASA/Cur-coloaded mPEG-PLGA nanoformulation and characterized it in detail.

We evaluated its potential in suppressing the growth of ovarian carcinoma in vitro and studied their possible synergistic effects on cancer therapy. The molecular mechanisms were further researched.

Materials and methods

Materials

Cur, SH-ASA, and 3-(4,5-dimethylthiazol-2-yl)-2,5-diphenyl tetrazolium bromide (MTT) were purchased from Sigma-Aldrich Co. (St Louis, MO, USA). Dulbecco's Modified Eagle's Medium (DMEM), Roswell Park Memorial Institute (RPMI)-1640 medium, and fetal bovine serum (FBS) were purchased from Gibco® (Thermo Fisher Scientific, Waltham, MA, USA). Ethyl acetate, methanol, and other organic solvents were purchased from ChengDu KeLong Chemical Co., Ltd. (Chengdu, People's Republic of China). The mPEG-PLGA copolymer with the designed molecular weight of 7,000 Da was previously synthesized in our lab. ES-2 human ovary clear cell carcinoma and SKOV3 human ovarian carcinoma cell lines were purchased from the American Type Culture Collection (Manassas, VA, USA). No ethics statement was required from the institutional review board for the use of these cell lines.

Preparation of mPEG-PLGA nanoparticles

mPEG-PLGA nanoparticles loaded with both SH-ASA and Cur, or each drug alone, were prepared using a modified o/w single-emulsion solvent evaporation process.[40] Briefly, the predetermined amounts of SH-ASA and Cur and

mPEG-PLGA polymer were dissolved in ethyl acetate, and the obtained solution was added slowly into aqueous phase, which consisted of distilled water and polyvinyl alcohol (1% m/v). The organic phase was emulsified with the aqueous phase by sonication using a microtip probe sonicator (JY88-II ultrasonic processor) at an output of 70 W for 2 minutes in an ice bath. The organic mixture was removed by vacuum rotary evaporation at 37°C for colloidal suspension, which was finally filtered through a 0.45 μm nylon filter to remove the unloaded SH-ASA and Cur.

In this study, the effect of different process parameters on the nanoparticles' mean diameter, polydispersity index (PDI), drug entrapment efficiencies (EE), and drug loading (DL) were assessed, including the feeding ratio of drug/mPEG-PLGA (w/w), mPEG-PLGA concentration in the organic phase, and types of organic solvent. The stabilities of different prescriptions were conducted through visual observations of sedimentation or creaming over a period of time. Unless specifically mentioned, all of the preparation processes were conducted by varying only one of the parameters, while keeping constant all the other process parameters at a set of standard conditions: 25 mg/mL of mPEG-PLGA, 1 mg of SH-ASA, and 250 μg of Cur in 1 mL of ethyl acetate as the organic phase (W/W =20:4:1); and 3 mL of 1% polyvinyl alcohol solution as the aqueous phase. The feeding ratio of drug/polymer was 1:20. SH-ASA-loading mPEG-PLGA nanoparticles and Cur-loading mPEG-PLGA nanoparticles were prepared in the same method. All batches of nanoparticles were prepared in triplicate.

Characterization of mPEG-PLGA nanoparticles

The concentrations of SH-ASA and Cur were determined by high-performance liquid chromatography (HPLC) (LC-20AD; Shimadzu Corporation, Tokyo, Japan) equipped with a column oven (CTO-20A), a plus autosampler (SIL-20AC), and a diode array detector (SPD-M20A). Chromatographic separations were performed on a Dionex Acclaim® 120 reversed-phase C_{18} column (Dionex Corporation, Sunnyvale, CA, USA) (250×4.6 mm) and the column temperature was kept at 30°C. The mobile phase was composed of 68:32 (v/v) acetonitrile–water with a flow rate of 1 mL/minute and the detection wavelength was set at 435 nm (Cur) and 254 nm (SH-ASA). The DL and EE of the SH-ASA/Cur nanoparticles were determined by dissolving 100 μL of colloidal suspension samples into 400 μL of methanol and performed on HPLC. The DL and EE were calculated using the following formulas:

$$DL = \frac{\text{Weight of drug in nanoparticle}}{\text{Weight of feeding polymer and drug}} \times 100\%, \quad (1)$$

and

$$EE = \frac{\text{Weight of drug in nanoparticle}}{\text{Weight of drug feeded}} \times 100\%. \quad (2)$$

The zeta potential and size distribution spectras of SH-ASA/Cur-loaded mPEG-PLGA nanoparticles were determined using a Zetasizer Nano ZS90 laser particle size analyzer (Malvern Instruments, Malvern, UK) at 25°C. The nanoparticle suspension was diluted five times before the measurement. During the process, the refractive index was 1.5000, and the temperature was kept at 25°C. Each test was measured three times and the mean value was taken.

A transmission electron microscope (TEM) was used to observe the morphology of the prepared nanoparticles. Nanoparticles were diluted three times with distilled water and placed on a copper grid covered with nitrocellulose. The sample was negatively stained with phosphotungstic acid and dried at room temperature, after which the TEM images were taken by a TEM (H-6009IV; Hitachi Ltd., Tokyo, Japan).

The thermal properties of free drugs and mPEG-PLGA nanoparticles were studied on a differential scanning calorimeter (DSC) (DSC F1 204 Phoenix®; Erich NETZSCH GmbH & Co. Holding KG, Selb, Germany). Samples were heated from 10°C–200°C under a nitrogen atmosphere at a heating rate of 10°C/minute. The DSC curves were recorded and analyzed.

In vitro release study

The in vitro drug release behavior of SH-ASA/Cur-coloaded mPEG-PLGA nanoparticles was determined using a modified dialysis method. Briefly, the SH-ASA/Cur-coloaded nanoparticles were placed in dialysis tubes (cutoff Mn =3 kDa), and the dialysis tubes were incubated in phosphate buffered saline buffer (pH =7.4) containing 0.5% (w/w) of Tween-80 at 37°C with gentle shaking. At specific time points, release media were collected and replaced by fresh media. The concentration of SH-ASA and Cur in the release media was determined using HPLC. All results were the mean of the three samples, and all data were expressed as the mean ± standard deviation.

Analysis of cytotoxicity

The cytotoxicity of free Cur, SH-ASA, and the drug-loaded mPEG-PLGA nanoparticles to the ES-2 and SKOV3 cell lines were evaluated by the MTT method. Briefly, ES-2

and SKOV3 cells were plated at a density of 5×10^3 cells per well in 100 μL of DMEM containing 10% FBS in 96-well plates and grown for 24 hours. Cells were then exposed to a series of free Cur, SH-ASA, or drug-loaded mPEG-PLGA nanoparticles at different concentrations for 48 hours. The viability of cells was measured using the MTT method. Results were the mean of six test runs. The combined indexes for the SH-ASA/Cur combination at different mass ratios were calculated as previously reported.[41]

In vitro cell uptake

The cellular uptake tests of the free SH-ASA, free Cur, and SH-ASA/Cur-coloaded nanoparticles were performed in ES-2 and SKOV3 cells by fluorescence microscope. Briefly, 3×10^5 cells were placed in each well of six-well plates and grown for 24 hours in 2 mL of DMEM medium (ES-2 were incubated in RPMI-1640 medium) supplemented with 10% FBS, penicillin (100 U/mL), and streptomycin (100 U/mL) at 37°C in 5% CO_2. Free SH-ASA/Cur or SH-ASA/Cur-coloaded nanoparticles were added to predesigned wells and incubated for 3 hours at 37°C in 5% CO_2. Then, the cells were stained with 100 μL of DAPI (5 μg/mL in phosphate buffered saline) for 10 minutes. After incubation, the growth media were removed, and the cells were washed with physiological saline for a total of three times. Fluorescence and light microscope (Olympus IX71; Olympus Corporation, Tokyo, Japan) were used to observe the fluorescence from DAPI and Cur that entered into the tumor cells.

Western blot analysis

Cellular proteins were extracted using RIPA (radioimmunoprecipitation assay) buffer (Beijing Solarbio Science & Technology Co., Ltd., Beijing, People's Republic of China) (50 mM Tris/HCl, pH 7.4, 150 mM NaCl 1% [v/v] NP-40, 0.1% [w/v] sodium dodecyl sulfate [SDS]) containing 1% (v/v) PMSF (Beijing Solarbio Science & Technology Co., Ltd.), 0.3% (v/v) protease inhibitor (Sigma-Aldrich Co.), and 0.1% (v/v) phosphorylated proteinase inhibitor (Sigma-Aldrich Co.). Lysates were centrifuged at 12,000 rpm at 4°C for 15 minutes, and the supernatant was collected for total protein. A bicinchoninic acid protein assay kit (Thermo Fisher Scientific) was used to determine the protein concentration. Equal amounts of protein (15 μg) were separated on an SDS–polyacrylamide gel electrophoresis gel (10% [v/v] polyacrylamide) and transferred onto a polyvinylidene fluoride membrane. Nonspecific binding was blocked using 8% (w/v) milk in Tris-buffered saline and Tween-20 (TBS-T) for 2 hours at room temperature. The membranes were then incubated with primary antibodies (ab7977 for Bax; ab7973 for Bcl-2; ab53056 for cytochrome c; ab32068 for procaspase-9; sc-56073 for caspase-9; and ab2302 for caspase-3) overnight at 4°C. All antibodies were applied according to the manufacturer's instructions. After several washes with TBS-T, the membranes were incubated in horseradish peroxidase-conjugated goat antirabbit and antimouse immunoglobulin (Ig)G or horseradish peroxidase-conjugated mouse antigoat IgG (Abmart, Berkeley Heights, NJ, USA) (all at a 1:5,000 dilution) for 2 hours at room temperature, and then washed with TBS-T. The target proteins were visualized using enhanced chemiluminescence (EMD Millipore, Billerica, MA, USA) according to the manufacturer's protocol, and quantified using density analysis normalized against β-actin to the manufacturer's recommendations.

Apoptosis detection

The cellular apoptosis was observed via Annexin V–fluorescein isothiocyanate (FITC) and propidium iodide staining. Briefly, SKOV3 cells were seeded into six-well plates and exposed to a series of nanoparticles separately. Cells treated with normal saline were marked as the control group. For Annexin V-FITC and propidium iodide staining, the treated cells were collected, washed, and then stained at room temperature for 15 minutes. The percentage of apoptotic cells was analyzed by flow cytometry (BD, Franklin Lakes, NJ, USA).

Statistical analysis

Data were expressed as the mean value ± standard deviation. Statistical analysis was performed with one-way analysis of variance using SPSS software. P-values <0.05 were considered to be statistically significant.

Results

Preparation and characterization of SH-ASA/Cur-coloaded mPEG-PLGA nanoparticles

In this work, SH-ASA/Cur-coloaded mPEG-PLGA nanoparticles (Figure 2) were successfully prepared through a modified o/w single-emulsion solvent evaporation process. To study the effects of the process parameters on the properties of the resultant nanoparticles, the drug/polymer mass ratio in feed, mPEG-PLGA concentration, and types of organic solvent were studied (Table 1). According to our results, under the same drug/mPEG-PLGA mass ratio, chloroform, dichloromethane, and ethyl acetate all resulted in high EE (>80%), while the nanoparticles prepared in ethyl acetate

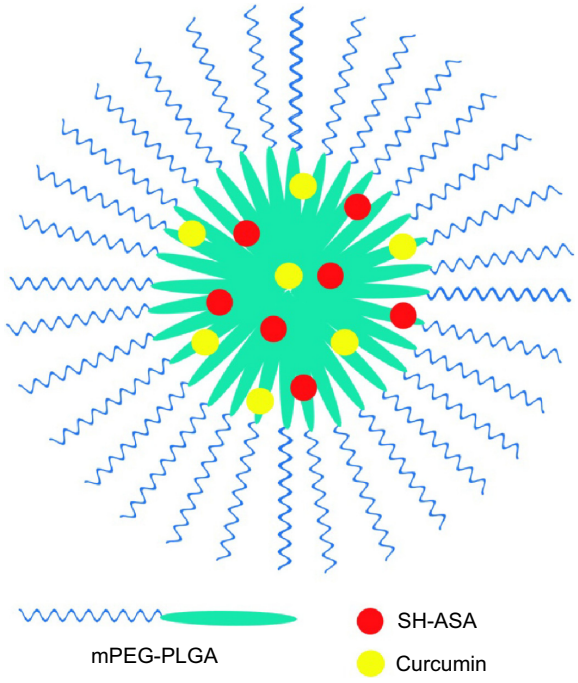

Figure 2 Structure of an SH-ASA/curcumin-coloaded mPEG-PLGA nanoparticle.
Abbreviations: mPEG-PLGA, methoxy poly(ethylene glycol)-poly (lactide-cogly-colide); SH-ASA, SH-aspirin.

had the smallest particle size and the highest stability than the other two. Different drug/mPEG-PLGA mass ratios in feed also obviously influenced the properties of the resultant nanoparticles. When using ethyl acetate as an organic solvent, the drug/mPEG-PLGA mass ratio of 1:30 demonstrated the highest encapsulation efficiency for both SH-ASA and Cur. This ratio also resulted in the smallest particle size and the highest stability, while its DL rate was lower than that of the other two. As a result, we chose 1/20 as the drug/mPEG-PLGA mass ratio in feed and ethyl acetate as the organic solvent in our following protocol to gain the ideal drug encapsulation efficiency, size distribution, DL, and stability for codelivery.

The sample S3 was characterized in detail, and its prescription was used for future applications. The encapsulation efficiency for SH-ASA and Cur was 83.17%±3.04% and 87.3%±3.68%, separately, with a total DL efficiency of 4.03%±0.05%. Moreover, these SH-ASA/Cur nanoparticles were monodisperse (PDI =0.179±0.016) in water with an average particle size of 122.3±6.8 nm. In Figure 3A, the particle size distribution spectrum of freshly prepared SH-ASA/Cur mPEG-PLGA nanoparticles was presented; this indicated that the SH-ASA/Cur nanoparticles had a very narrow particle size distribution. Meanwhile, the zeta potential spectrum demonstrated that the nanoparticles were neutral (Figure 3B). According to the TEM image of SH-ASA/Cur nanoparticles (Figure 3C), these nanoparticles were spherical and monodisperse with a mean diameter of ~100 nm.

To examine the crystallinity of the nanoparticle-encapsulated drugs, the DSC analysis was performed on different formulations of SH-ASA and Cur. In Figure 4A, the DSC curves were shown. Compared to the free drug/drug-loaded nanoparticle mixtures, the melting transition peaks of Cur or SH-ASA did not appear in the DSC curves of Cur nanoparticles, SH-ASA nanoparticles, or SH-ASA/Cur-coloaded nanoparticles. This confirmed that there were no Cur or SH-ASA crystals in the SH-ASA/Cur mPEG-PLGA nanoparticles, suggesting that Cur and SH-ASA were molecularly incorporated in the mPEG-PLGA nanoparticles.

Release profile in vitro

To confirm whether Cur and SH-ASA could be released from the drug loaded mPEG-PLGA nanoparticles, the release profiles of Cur and SH-ASA from the mPEG-PLGA nanoparticles were studied using a dialysis method in vitro. Our results indicate that SH-ASA/Cur-loaded mPEG-PLGA nanoparticles could release Cur and SH-ASA slowly (Figure 4B). According to our results, about 55.2% of the total Cur and 58.9% of the total SH-ASA was released in 7 days, demonstrating an obvious slow-release behavior.

Table 1 Characterization of the prepared SH-ASA/Cur nanoparticles

Sample	Solvent	Drug: polymer[a]	EEA (%)	EEC (%)	Size (nm)	PDI	DLA (%)	DLC (%)	Stability
S1	Chloroform	1:20	80±3.12	92.76±4.56	387.6±31.3	0.418±0.047	3.09±0.08	0.93±0.01	2 hours
S2	Dichloromethane	1:20	92.65±4.26	90.84±4.23	284±18.6	0.286±0.028	3.51±0.06	0.90±0.02	24 hours
S3	Ethyl acetate	1:20	83.17±3.04	87.3±3.68	122.3±6.8	0.179±0.016	3.15±0.05	0.88±0.05	72 hours
S4	Ethyl acetate	1:5	35.06±2.76	40.74±2.45	271.6±13.6	0.402±0.02	5.12±0.13	1.65±0.11	<10 minutes
S5	Ethyl acetate	1:10	70.82±4.43	79.71±5.88	172.2±8.8	0.276±0.012	5.38±0.14	1.53±0.09	4 hours
S7	Ethyl acetate	1:30	89.56±3.56	94.12±3.14	107.1±2.3	0.171±0.016	2.21±0.05	0.74±0.02	>96 hours

Notes: [a]In feed; Data is presented as mean ± standard deviation.
Abbreviations: SH-ASA, SH-aspirin; Cur, curcumin; EEA, entrapment efficiency of aspirin; EEC, entrapment efficiency of curcumin; PDI, polydispersity index; DLA, drug-loading efficiency of aspirin; DLC, drug-loading efficiency of curcumin.

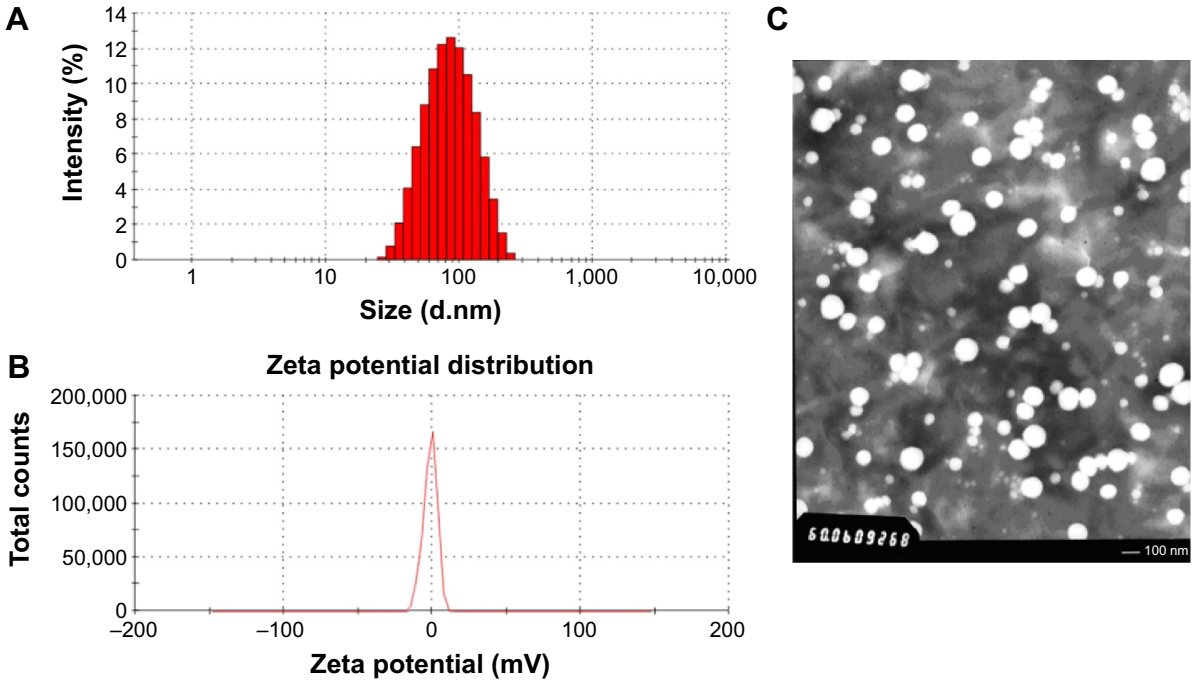

Figure 3 Characterization of SH-ASA/Cur-coloaded mPEG-PLGA nanoparticles.
Notes: (**A**) Size distribution; (**B**) zeta potential; (**C**) TEM image.
Abbreviations: SH-ASA, SH-aspirin; Cur, curcumin; mPEG-PLGA, methoxy poly(ethylene glycol)-poly (lactide-coglycolide); TEM, transmission electron microscope.

Cellular uptake

The cellular uptake of SH-ASA/Cur mPEG-PLGA nanoparticles was compared with that of free SH-ASA and Cur in vitro. After SKOV3 and ES-2 cancer cells were exposed to free drugs or to the SH-ASA/Cur-coloaded mPEG-PLGA nanoparticles for 3 hours, the cells were collected for the analysis of Cur and DAPI-derived fluorescence by microscope. As shown in Figures 5 and 6, when SKOV3 and ES-2 cells were incubated, the cellular fluorescence intensities in the SH-ASA/Cur-coloaded mPEG-PLGA nanoparticle-treated groups were higher than those in the cells incubated with the same dosage of the free SH-ASA/Cur combination

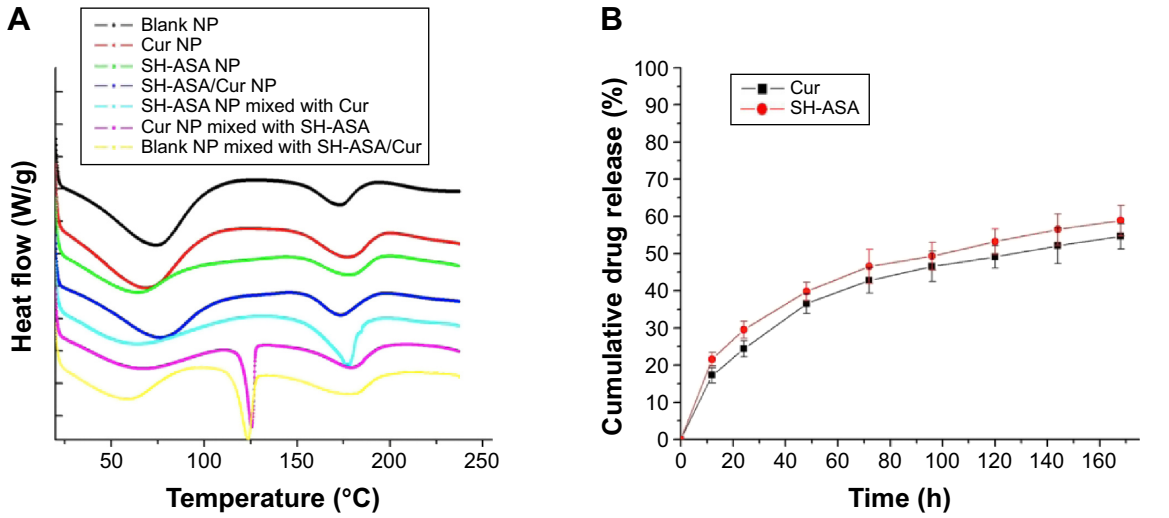

Figure 4 Characterization of SH-ASA/Cur-coloaded mPEG-PLGA NPs.
Notes: (**A**) DSC curves of blank NPs, Cur NPs, SH-ASA NPs, SH-ASA/Cur-coloaded NPs, SH-ASA NPs physically mixed with free Cur, Cur NPs mixed with free SH-ASA, and blank NPs mixed with both free drugs. (**B**) In vitro drug release behaviors of SH-ASA/Cur-coloaded mPEG-PLGA NPs.
Abbreviations: NP, nanoparticle; Cur, curcumin; SH-ASA, SH-aspirin; h, hours; mPEG-PLGA, methoxy poly(ethylene glycol)-poly (lactide-coglycolide); DSC, differential scanning calorimeter.

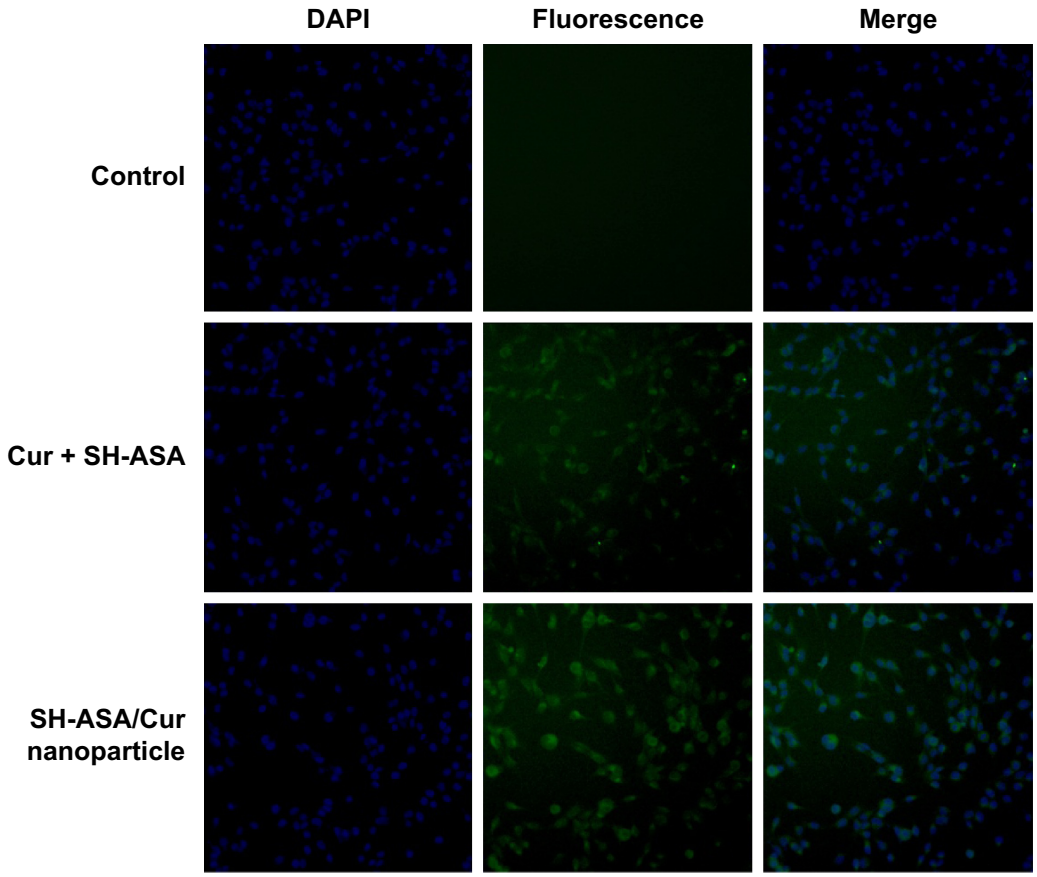

Figure 5 Uptake by SKOV3 cells.
Abbreviations: DAPI, 4′,6-diamidino-2-phenylindole; Cur, curcumin; SH-ASA, SH-aspirin.

groups. Thus, it is suggested that the incorporation of SH-ASA and Cur in mPEG-PLGA nanoparticles increased their cellular uptake.

Anticancer activity in vitro

First, the cytotoxicity of free SH-ASA and Cur on ES-2 and SKOV3 ovarian cancer cells was studied in vitro, and results are presented in Figure 7. According to our results, both Cur and SH-ASA could kill cancer cells, while the former showed higher efficiency. The IC_{50}s of Cur were 7.8 μg/mL and 6.9 μg/mL on ES-2 and SKOV3 cell lines, respectively, and those for SH-ASA were 56.1 μg/mL and 52.5 μg/mL, respectively. We then evaluated the possible synergistic anticancer effects of the free Cur and SH-ASA combinations on the SKOV3 cell lines. In this study, SH-ASA was combined with 5 μg/mL of Cur at different ratios (1:1, 1:2, 1:4, and 1:6), separately. The combination treatment showed obvious synergistic antiproliferation effects on SKOV3 cells at the ratios of 1:4 and 1:6 (Figure 8). In these two groups, cell survival rates were much lower than either in the free Cur or free SH-ASA groups. Moreover, it could be observed that those synergistic effects increased along with the increase of the SH-ASA amount. In order to further evaluate the drug interactions in combination chemotherapy, their combination indexes (CI) were calculated. The CI for the SH-ASA and Cur combined therapy on SKOV3 cells at different ratios (1:1, 1:2, 1:4, and 1:6) was 1.09, 1.13, 0.78, and 0.95, respectively, and the CI for the ES-2 cells were 1.10, 1.16, 0.83, and 0.98, respectively. As previously reported, CI values less than 1 indicate synergy,[41] suggesting that the 1:4 ratio has the strongest synergistic effect among them all.

In order to address the poor water solubility issue of Cur and SH-ASA, we used the mPEG-PLGA nanoparticles to encapsulate them and prepared the SH-ASA/Cur-coloaded mPEG-PLGA nanoparticles. The anticancer abilities of SH-ASA/Cur-encapsulated nanoparticles (the SH-ASA/Cur mass ratio was 4:1; the total drug concentration was 5.62–60 μg/mL) on both the SKOV3 and ES-2 cell lines were then studied. According to our results, the SH-ASA/Cur-coloaded mPEG-PLGA nanoparticles showed strong anticancer effects in an obvious concentration-dependent

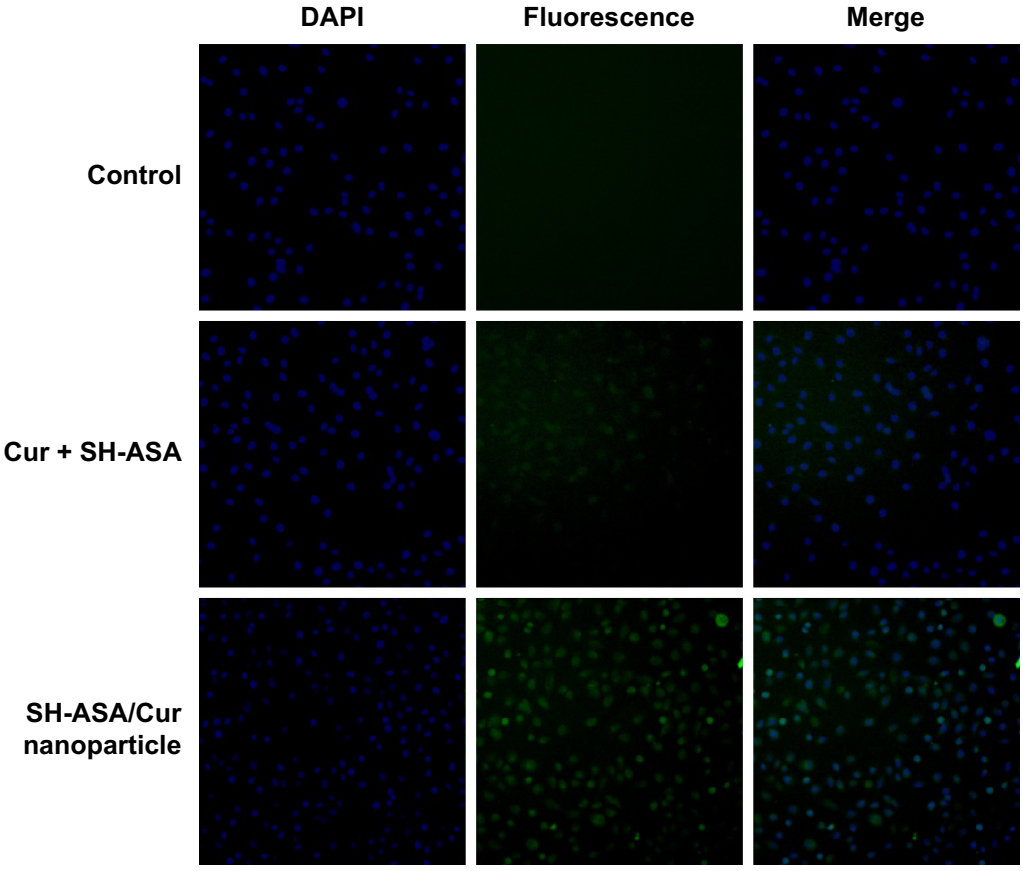

Figure 6 Uptake by ES-2 cells.
Abbreviations: DAPI, 4′,6-diamidino-2-phenylindole; Cur, curcumin; SH-ASA, SH-aspirin.

manner (Figure 9). The coloaded nanoparticles showed better anticancer effects than Cur nanoparticles or SH-ASA nanoparticles alone on both SKOV3 and ES-2 cells, which might be due to these synergistic effects. Besides, the SH-ASA/Cur-coloaded mPEG-PLGA nanoparticles had similar anticancer abilities to the free SH-ASA/Cur combination. Our results indicated that encapsulation of the two drugs by the mPEG-PLGA nanoparticles not only retained their cancer-controlling ability, but these drugs also demonstrated a synergistic effect when administered together through codelivery.

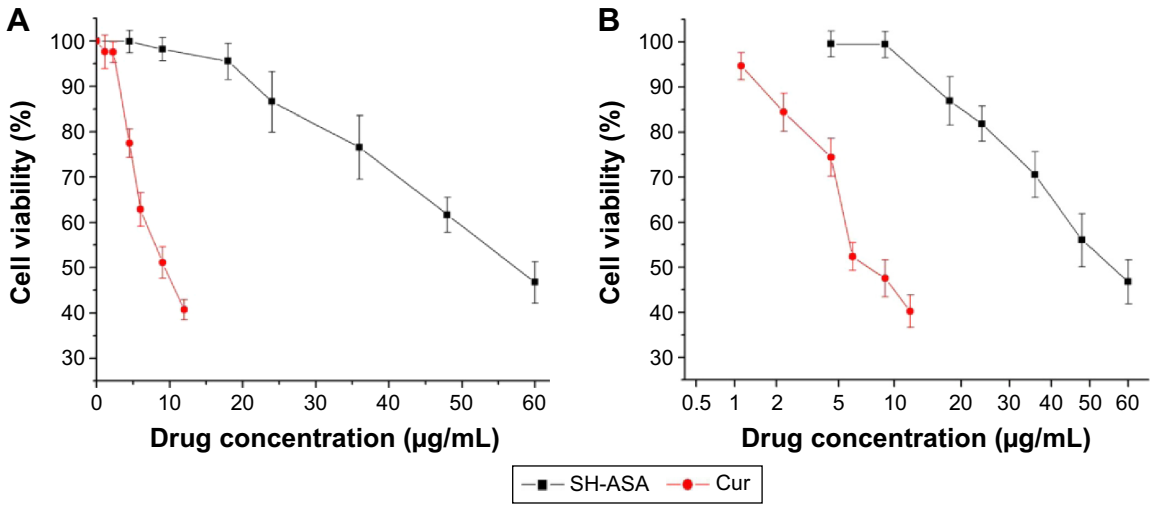

Figure 7 Anticancer abilities of free SH-ASA and Cur on ES-2 and SKOV3 human ovarian cancer cells in vitro.
Notes: (**A**) ES-2 cells; (**B**) SKOV3 cells.
Abbreviations: SH-ASA, SH-aspirin; Cur, curcumin.

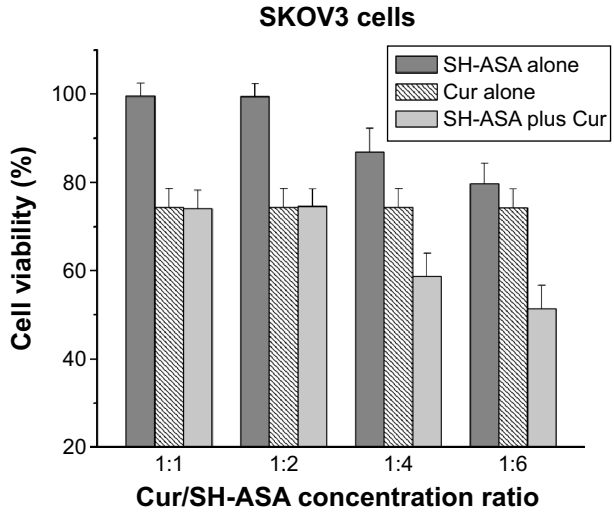

Figure 8 Anticancer effect of free SH-ASA and Cur combination.
Note: The results of the 1:4 and 1:6 combination groups demonstrated obvious synergistic effects.
Abbreviations: SH-ASA, SH-aspirin; Cur, curcumin.

SH-ASA/Cur-coloaded mPEG-PLGA nanoparticles induced apoptosis in human ovarian cancer cells

To determine whether the SH-ASA/Cur nanoparticle-induced loss of the proliferation capacity and cell viability of human ovarian cancer cells was associated with the induction of apoptosis, SKOV3 cells were treated with SH-ASA nanoparticles (SH-ASA concentration: 18 μg/mL), Cur nanoparticles (Cur concentration: 4.5 μg/mL), and SH-ASA/Cur-coloaded mPEG-PLGA nanoparticles (18 μg/mL for SH-ASA and 4.5 μg/mL for Cur). The numbers of apoptotic cells were assessed using flow cytometry. As shown in Figure 10, after 48 hours of treatment, the early apoptosis rates (Q4 region) of the SH-ASA nanoparticle- and Cur nanoparticle-treated cells were 7% and 32.84%, respectively, while that of the SH-ASA/Cur-loaded mPEG-PLGA nanoparticle group was 64.7%. The later apoptosis rates (Q2 region) of the SH-ASA nanoparticle- and Cur nanoparticle-treated cells were 6.9% and 19.8%, respectively, while that of the SH-ASA/Cur-loaded mPEG-PLGA nanoparticle group was 21%. Both the early and later apoptosis data indicated that SH-ASA/Cur-loaded mPEG-PLGA nanoparticles had stronger apoptosis-inducing ability. The apoptosis assay results were consistent with the MTT results described earlier, demonstrating obvious synergistic effects between Cur and SH-ASA, and suggesting that inducing apoptosis is a possible mechanism for cytotoxicity.

We further studied the possible anticancer mechanism by Western blotting. The protein-level analyses results suggested that the observed apoptosis might be induced by triggering the mitochondria-dependent apoptotic signaling pathway. As shown in Figure 11, when compared to the Cur mPEG-PLGA nanoparticles, the SH-ASA/Cur-coloaded mPEG-PLGA nanoparticles obviously increased the cytochrome c levels in SKOV3 cells, which is a critical step in the mitochondrial-dependent signaling pathways of apoptosis.[42] In the meantime, when compared to the Cur nanoparticles alone, treatment with SH-ASA/Cur-coloaded mPEG-PLGA nanoparticles resulted in an obvious reduction in the levels of the antiapoptotic protein Bcl-2, with an obvious increase in the levels of proapoptotic protein, Bax. After treatment with the SH-ASA/

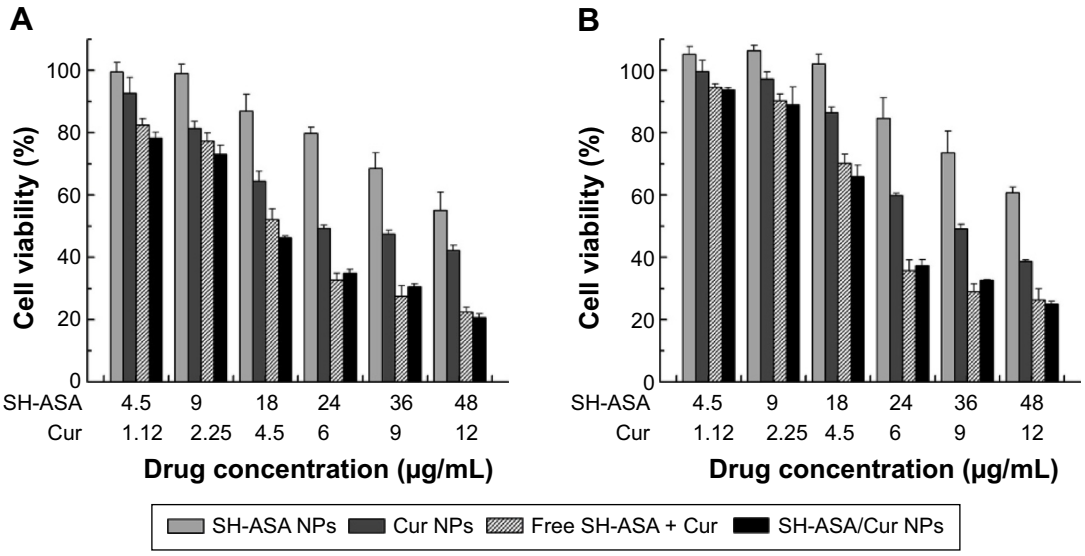

Figure 9 Anticancer abilities of different formulations containing SH-ASA and/or Cur against SKOV3 and ES-2 cells after treatment for 48 hours.
Notes: (**A**) SKOV3 cells; (**B**) ES-2 cells.
Abbreviations: SH-ASA, SH-aspirin; NPs, nanoparticles; Cur, curcumin.

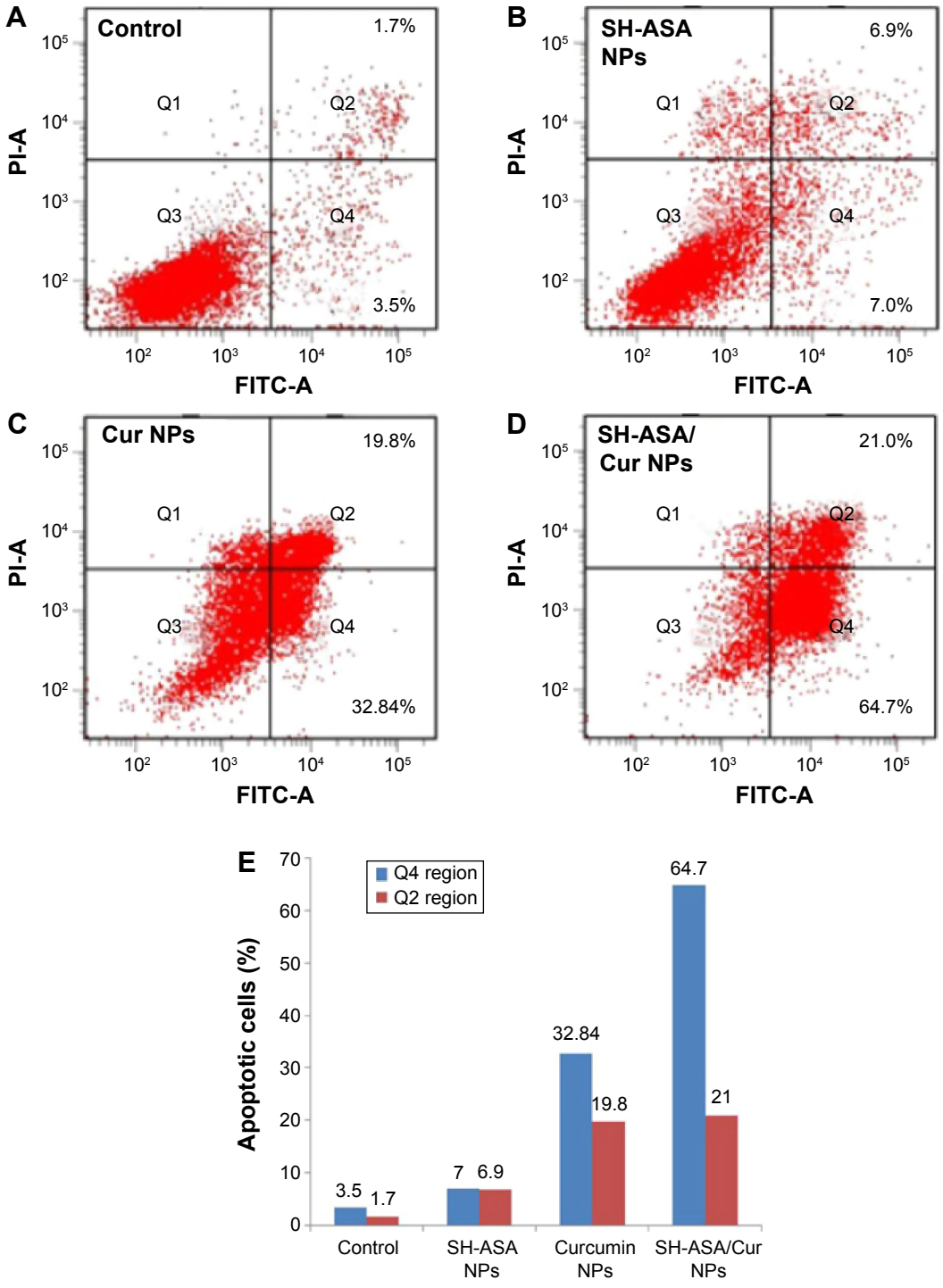

Figure 10 SH-ASA/Cur-coloaded mPEG-PLGA NPs induced apoptosis in human ovarian cancer cells.
Notes: (**A**) Control; (**B**) SH-ASA NPs; (**C**) Cur NPs; (**D**) SH-ASA/Cur NPs; (**E**) the early (Q4 region) and later (Q2 region) apoptosis rates of different formulations.
Abbreviations: FITC-A, Annexin V–fluorescein isothiocyanate; SH-ASA, SH-aspirin; NPs, nanoparticles; Cur, curcumin; mPEG-PLGA, methoxy poly(ethylene glycol)-poly (lactide-coglycolide).

Cur-coloaded mPEG-PLGA nanoparticles, increased protein levels of caspase-9 and caspase-3 were observed, while the expression of procaspase-9 decreased. This indicated that the codelivery nanoparticles had stronger effects on activating the mitochondrial-based apoptosis pathway than did the single-drug formulation. Our results suggested that apoptosis activation might be a possible explanation for the synergistic anticancer effects of the coloaded nanoparticles.

Discussion

SH-ASA and Cur are potential anticancer agents, but their hydrophobicity and low efficiency limited their development

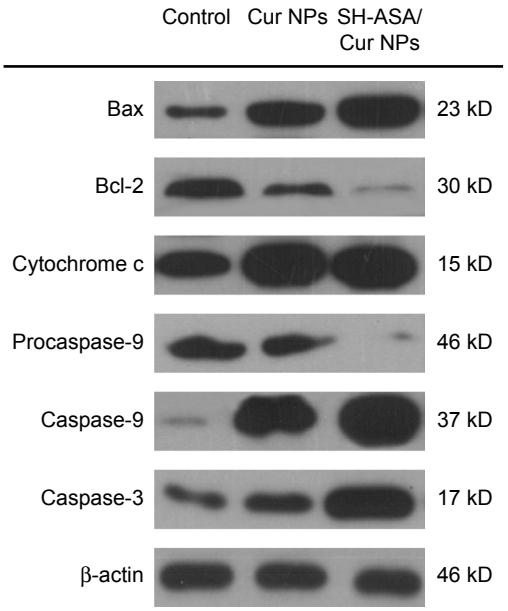

Figure 11 SH-ASA/Cur-codelivery mPEG-PLGA nanoparticles demonstrated a stronger effect when activating the mitochondrial-based apoptosis signaling pathway than did the single-drug formulation, suggesting that this might be a possible explanation for the synergistic anticancer effects.
Abbreviations: Cur, curcumin; NPs, nanoparticles; SH-ASA, SH-aspirin; mPEG-PLGA, methoxy poly(ethylene glycol)-poly (lactide-coglycolide).

and application. Nanotechnology provides effective methods for optimizing the water solubility issue of hydrophobic drugs. Besides, the combination of the two agents might improve their therapeutic potentials through synergistic effects. In this study, SH-ASA and Cur were coencapsulated into mPEG-PLGA nanoparticles through a modified o/w single-emulsion solvent evaporation process, creating SH-ASA/Cur-coloaded mPEG-PLGA nanoparticles. The prepared nanoparticles had a mean particle size of 122.3±6.8 nm and were monodispersed (PDI =0.179±0.016) in water solutions. The obtained nanoparticles were neutral. Zeta potential is a key parameter that is widely used to predict suspension stability. It is well known that the higher the zeta potential, the more stable the nanoparticle. However, the mPEG segment in the mPEG-PLGA nanoparticles also plays a role as a nonionic stabilizer, which provides steric stabilization that is dominated by a solvation effect.[43] In the nanoparticle, the encapsulation efficiencies of SH-ASA and Cur were 83.17%±3.04% and 87.3%±3.68%, separately, with a DL rate of 4.03%±0.05%. After encapsulation, SH-ASA and Cur were molecularly dispersed in the PLGA core of mPEG-PLGA nanoparticles, and they could be slowly released from the particle in vitro. Moreover, the SH-ASA/Cur-coloaded mPEG-PLGA nanoparticles retained the cytotoxicity of Cur and SH-ASA on the ES-2 and SKOV3 human ovarian carcinoma cells in vitro, demonstrating better anticancer ability than either SH-ASA or Cur nanoparticles alone, showing a synergistic effect. Our results further suggested that the combination of SH-ASA and Cur more obviously induced apoptosis in SKOV3 cells by triggering the mitochondrial signaling pathway. In conclusion, SH-ASA/Cur-coloaded mPEG-PLGA nanoparticles provide an excellent aqueous formulation for SH-ASA and Cur. The combination of the two agents showed a strong synergistic effect in inhibiting the growth of ovarian carcinoma cells through the induction of apoptosis.

Cur is recognized as an efficient and safe anticancer agent.[6,7,10,12,13,44] However, Cur is water insoluble, which greatly limits its clinical administration. Thus, developing better aqueous formulations for Cur delivery attracts much attention. HS-NSAIDs have been reported recently to have potential cancer-controlling bioactivity.[29–32] Their difficulties in water solubility also limit further development. Nanotechnology provides optimizing strategies when solving the issue of poor water solubility of hydrophobic drugs. Moreover, as a promising drug-delivery platform, polymeric nanoparticles have many advantages, such as a prolonged systemic circulation lifetime, reduced nonspecific cellular uptake, as well as multidrug encapsulation for combinatorial treatment.[45–49] In addition to delivering single therapeutics, there are growing interests in multiagent codelivery that can simultaneously incorporate and deliver multiple types of therapeutic payloads for combined therapy.[50–52] More importantly, these codelivery nanocarriers may potentially allow for the creation of synergetic effects to eventually improve overall treatment outcomes.[53,54] Recently, Zhu et al[49] reported using PLGA nanoparticles to codeliver docetaxel together with vitamin E TPGS, demonstrating their outstanding and optimized anticancer ability; Deng et al[54] coencapsulated a potent endogenous tumor-suppressive molecule, miR-34a, with doxorubicin into hyaluronic acid–chitosan nanoparticles, which were simultaneously delivered into breast cancer cells for improved therapeutic effects. In the aforementioned studies, different methods of formulation preparations, such as nanoprecipitation, were employed. In our study, we successfully used the mPEG-PLGA copolymer to coencapsulate Cur and SH-ASA through a modified o/w single-emulsion solvent evaporation process. In this process, Cur and SH-ASA were encapsulated in the core area of the core–shell-structured mPEG-PLGA nanoparticle. The DSC analyses indicated that the encapsulated Cur and SH-ASA were amorphous (Figure 4A). The obtained SH-ASA/Cur mPEG-PLGA nanoparticles were completely dispersed in aqueous solution with high stability, indicating the optimizing of solubility problems. In our work, the SH-ASA and Cur-coloaded mPEG-PLGA

nanoparticles were prepared using a simple single-emulsion solvent evaporation process, making it convenient for large-scale production. Besides, the obtained nanoparticles had a comparatively small particle size distribution and a high DL capacity. Moreover, the in vitro release behavior indicated their slow drug releasing property, which might further contribute to its safety, as well as to its drug metabolism. The small size and hydrophilic polyethylene glycol shell may also allow SH-ASA/Cur mPEG-PLGA-coloaded nanoparticles to circulate for a long time in vivo.[55,56] Thus, our results suggested that this SH-ASA/Cur mPEG-PLGA-coloaded nanoparticle is a good aqueous formulation for combination therapy.

In previous reports, both Cur and SH-ASA have demonstrated limited cancer-controlling capacity.[2–5,30,31] In order to gain better therapeutic activity, in the present study, we applied a combination therapy on ovarian cancer cells with SH-ASA/Cur-coloaded mPEG-PLGA nanoparticles. Compared to free drugs, the prepared nanoparticles not only retained the cytotoxicity of the two agents on the ES-2 and SKOV3 cells, but they also showed better anticancer ability than either the SH-ASA or Cur nanoparicles alone, suggesting a strong synergistic effect. Thus, our results indicated that the codelivery of SH-ASA and Cur via a nanocarrier might hold potential in cancer therapy. In reported studies, there have been many examples of applying Cur in combination therapies. Abouzeid et al[57] codelivered Cur and paclitaxel, and they observed a clear synergistic effect against SKOV-3TR cells. Carlson et al[58] found that the combination of resveratrol and Cur were also synergistic in inhibiting SKOV3 cell proliferation. In our study, the combination of Cur and SH-ASA resulted in increased apoptosis induction in cancer cells. Our Western blotting results suggested that the nanoparticle-delivered combination triggered the mitochondrial-based intrinsic apoptosis pathway by activating caspase-3 and caspase-9. This effect on the signaling pathway was much stronger than that of the Cur or SH-ASA nanoparticles alone, suggesting a possible synergistic mechanism. Pei et al[59] evaluated the anticancer ability of SH-releasing compound, sulforaphane, and showed that the released hydrogen sulfide mediated the anticancer properties through activation of the p38 mitogen-activated protein kinases and c-Jun N-terminal kinase. On the other hand, there is a high possibility that the imbalance of the reactive oxygen species/reactive nitrogen species system may lead to uncontrolled cell proliferation and cancer. The unbalanced system could modulate gene expression with numerous oncogenes and tumor-suppressor genes.[60] Under this circumstance, H_2S and H_2S containing prodrugs could act as pro-oxidants to induce a redox shift,[61–63] and they could also ruin the cancer cell's proliferative machinery. Furthermore, many redox-targeted cancer drugs, such as H_2S-releasing agents, are capable of potentiating the effect of other anticancer agents, adjusting the cancer cells' sensitization to cytotoxicity.[64] Thus, as one of the H_2S donors, SH-ASA might also induce a redox shift in tumor cells, contributing to the synergistic effect when combined with Cur in our study.

Conclusion

SH-ASA/Cur-coloaded mPEG-PLGA nanoparticles were prepared through a modified o/w single-emulsion solvent evaporation process. Coencapsulation of SH-ASA and Cur makes them nanodipersed in a water solution, overcoming solubility drawbacks. The prepared SH-ASA/Cur-coloaded mPEG-PLGA nanocarriers showed a small size, slow-releasing behavior, high DL capacity, and stability. Obvious synergistic anticancer effects on ES-2 and SKOV3 human ovarian carcinoma cells were obtained in vitro through coencapsulation. It is further suggested that the combination of SH-ASA and Cur induced cell apoptosis through the mitochondrial-based signaling pathway. Our results demonstrated that SH-ASA/Cur-coloaded mPEG-PLGA nanoparticles hold potential clinical applications in ovarian cancer therapy.

Acknowledgments

This work was supported by the Foundation for Sichuan Distinguished Young Academic and Technology Leaders (2012JQ0014) and the National Natural Science Foundation of China (grant number: 31070815).

Disclosure

The authors report no conflicts of interest in this work.

References

1. Jemal A, Bray F, Center MM, Ferlay J, Ward E, Forman D. Global cancer statistics. *CA Cancer J Clin*. 2011;61(2):69–90.
2. Vaughan S, Coward JI, Best RC Jr, et al. Rethinking ovarian cancer: recommendations for improving outcomes. *Nat Rev Cancer*. 2011; 11(10):719–725.
3. Egan ME, Pearson M, Weiner SA, et al. Curcumin, a major constituent of turmeric, corrects cystic fibrosis defects. *Science*. 2004; 304(5670):600–602.
4. Goel A, Kunnumakkara AB, Aggarwal BB. Curcumin as "Curecumin": from kitchen to clinic. *Biochem Pharmacol*. 2008;75(4):787–809.
5. Jagetia GC, Aggarwal BB. "Spicing up" of the immune system by curcumin. *J Clin Immunol*. 2007;27(1):19–35.
6. Maheshwari RK, Singh AK, Gaddipati J, Srimal RC. Multiple biological activities of curcumin: a short review. *Life Sci*. 2006;78(18): 2081–2087.
7. Li L, Braiteh FS, Kurzrock R. Liposome-encapsulated curcumin: in vitro and in vivo effects on proliferation, apoptosis, signaling, and angiogenesis. *Cancer*. 2005;104(6):1322–1331.

8. Choudhuri T, Pal S, Agwarwal ML, Das T, Sa G. Curcumin induces apoptosis in human breast cancer cells through p53-dependent Bax induction. *FEBS Lett*. 2002;512(1–3):334–340.
9. Dorai T, Cao YC, Dorai B, Buttyan R, Katz AE. Therapeutic potential of curcumin in human prostate cancer. III. Curcumin inhibits proliferation, induces apoptosis, and inhibits angiogenesis of LNCaP prostate cancer cells in vivo. *Prostate*. 2001;47(4):293–303.
10. Rao CV, Rivenson A, Simi B, Reddy BS. Chemoprevention of colon carcinogenesis by dietary curcumin, a naturally occurring plant phenolic compound. *Cancer Res*. 1995;55(2):259–266.
11. Bharti AC, Donato N, Singh S, Aggarwal BB. Curcumin (diferuloylmethane) down-regulates the constitutive activation of nuclear factor-kappa B and IkappaBalpha kinase in human multiple myeloma cells, leading to suppression of proliferation and induction of apoptosis. *Blood*. 2003;101(3):1053–1062.
12. Tian B, Wang Z, Zhao Y, et al. Effects of curcumin on bladder cancer cells and development of urothelial tumors in a rat bladder carcinogenesis model. *Cancer Lett*. 2008;264(2):299–308.
13. Shi M, Cai Q, Yao L, Mao Y, Ming Y, Ouyang G. Antiproliferation and apoptosis induced by curcumin in human ovarian cancer cells. *Cell Biol Int*. 2006;30(3):221–226.
14. Clark CA, McEachern MD, Shah SH, et al. Curcumin inhibits carcinogen and nicotine-induced Mammalian target of rapamycin pathway activation in head and neck squamous cell carcinoma. *Cancer Prev Res (Phila)*. 2010;3(12):1586–1595.
15. Anand P, Nair HB, Sung B, et al. Design of curcumin-loaded PLGA nanoparticles formulation with enhanced cellular uptake, and increased bioactivity in vitro and superior bioavailability in vivo. *Biochem Pharmacol*. 2010;79(3):330–338.
16. Wilken R, Veena MS, Wang MB, Srivatsan ES. Curcumin: a review of anti-cancer properties and therapeutic activity in head and neck squamous cell carcinoma. *Mol Cancer*. 2011;10:12.
17. Aggarwal BB, Harikumar KB. Potential therapeutic effects of curcumin, the anti-inflammatory agent, against neurodegenerative, cardiovascular, pulmonary, metabolic, autoimmune and neoplastic diseases. *Int J Biochem Cell Biol.* 2009;41(1):40–59.
18. Aggarwal BB, Kumar A, Bharti AC. Anticancer potential of curcumin: preclinical and clinical studies. *Anticancer Res.* 2003;23(1A):363–398.
19. Shishodia S, Sethi G, Aggarwal BB. Curcumin: getting back to the roots. *Ann N Y Acad Sci.* 2005;1056:206–217.
20. Agrawal DK, Mishra PK. Curcumin and its analogues: potential anticancer agents. *Med Res Rev.* 2010;30(5):818–860.
21. Zhou H, Beevers CS, Huang S. The targets of curcumin. *Curr Drug Targets*. 2011;12(3):332–347.
22. Krishnan K, Ruffin MT, Normolle D, et al. Colonic mucosal prostaglandin E2 and cyclooxygenase expression before and after low aspirin doses in subjects at high risk or at normal risk for colorectal cancer. *Cancer Epidemiol Biomarkers Prev*. 2001;10(5):447–453.
23. Ruffin MT 4th, Krishnan K, Rock CL, et al. Suppression of human colorectal mucosal prostaglandins: determining the lowest effective aspirin dose. *J Natl Cancer Inst*. 1997;89(15):1152–1160.
24. Huang MT, Lou YR, Ma W, Newmark HL, Reuhl KR, Conney AH. Inhibitory effects of dietary curcumin on forestomach, duodenal, and colon carcinogenesis in mice. *Cancer Res*. 1994;54(22):5841–5847.
25. Profita M, Sala A, Bonanno A, et al. Chronic obstructive pulmonary disease and neutrophil infiltration: role of cigarette smoke and cyclooxygenase products. *Am J Physiol Lung Cell Mol Physiol*. 2010;298(2):L261–L269.
26. Sinicrope FA, Half E, Morris JS, et al; Familial Adenomatous Polyposis Study Group. Cell proliferation and apoptotic indices predict adenoma regression in a placebo-controlled trial of celecoxib in familial adenomatous polyposis patients. *Cancer Epidemiol Biomarkers Prev*. 2004;13(6):920–927.
27. Carroll RE, Benya RV, Turgeon DK, et al. Phase IIa clinical trial of curcumin for the prevention of colorectal neoplasia. *Cancer Prev Res (Phila)*. 2011;4(3):354–364.
28. Kashfi K. Anti-inflammatory agents as cancer therapeutics. *Adv Pharmacol*. 2009;57:31–89.
29. Chattopadhyay M, Kodela R, Olson KR, Kashfi K. NOSH-aspirin (NBS-1120), a novel nitric oxide- and hydrogen sulfide-releasing hybrid is a potent inhibitor of colon cancer cell growth in vitro and in a xenograft mouse model. *Biochem Biophys Res Commun*. 2012;419(3): 523–528.
30. Chattopadhyay M, Nath N, Kodela R, et al. Hydrogen sulfide-releasing aspirin inhibits the growth of leukemic Jurkat cells and modulates β-catenin expression. *Leuk Res*. 2013;37(10):1302–1308.
31. Chattopadhyay M, Kodela R, Nath N, et al. Hydrogen sulfide-releasing NSAIDs inhibit the growth of human cancer cells: a general property and evidence of a tissue type-independent effect. *Biochem Pharmacol*. 2012;83(6):715–722.
32. Chattopadhyay M, Kodela R, Nath N, Barsegian A, Boring D, Kashfi K. Hydrogen sulfide-releasing aspirin suppresses NF-κB signaling in estrogen receptor negative breast cancer cells in vitro and in vivo. *Biochem Pharmacol*. 2012;83(6):723–732.
33. Kodela R, Chattopadhyay M, Kashfi K. NOSH-Aspirin: A Novel Nitric Oxide-Hydrogen Sulfide-Releasing Hybrid: a new class of anti-inflammatory pharmaceuticals. *ACS Med Chem Lett*. 2012;3(3):257–262.
34. Zhang L, Chan JM, Gu FX, et al. Self-assembled lipid – polymer hybrid nanoparticles: a robust drug delivery platform. *ACS Nano*. 2008;2(8):1696–1702.
35. Gou M, Wei X, Men K, et al. PCL/PEG copolymeric nanoparticles: potential nanoplatforms for anticancer agent delivery. *Curr Drug Targets*. 2011;12(8):1131–1150.
36. Wang X, Yang L, Chen ZG, Shin DM. Application of nanotechnology in cancer therapy and imaging. *CA Cancer J Clin*. 2008;58(2):97–110.
37. Wen Y, Gallego MR, Nielsen LF, Jorgensen L, Møller EH, Nielsen HM. Design and characterization of core-shell mPEG-PLGA composite microparticles for development of cell-scaffold constructs. *Eur J Pharm Biopharm*. 2013;85(1):87–98.
38. Peng KT, Chen CF, Chu IM, et al. Treatment of osteomyelitis with teicoplanin-encapsulated biodegradable thermosensitive hydrogel nanoparticles. *Biomaterials*. 2010;31(19):5227–5236.
39. Acharya S, Sahoo SK. PLGA nanoparticles containing various anticancer agents and tumour delivery by EPR effect. *Adv Drug Deliv Rev*. 2011;63(3):170–183.
40. Song X, Zhao Y, Hou S, et al. Dual agents loaded PLGA nanoparticles: systematic study of particle size and drug entrapment efficiency. *Eur J Pharm Biopharm*. 2008;69(2):445–453.
41. Zhao L, Wientjes MG, Au JL. Evaluation of combination chemotherapy: integration of nonlinear regression, curve shift, isobologram, and combination index analyses. *Clin Cancer Res*. 2004;10(23):7994–8004.
42. Green DR, Reed JC. Mitochondria and apoptosis. *Science*. 1998;281(5381):1309–1312.
43. Wu L, Zhang J, Watanabe W. Physical and chemical stability of drug nanoparticles. *Adv Drug Deliv Rev*. 2011;63(6):456–469.
44. Gou M, Men K, Shi H, et al. Curcumin-loaded biodegradable polymeric micelles for colon cancer therapy in vitro and in vivo. *Nanoscale*. 2011;3(4):1558–1567.
45. Zhang Y, Tang L, Sun L, et al. A novel paclitaxel-loaded poly(epsilon-caprolactone)/Poloxamer 188 blend nanoparticle overcoming multidrug resistance for cancer treatment. *Acta Biomater*. 2010;6(6):2045–2052.
46. Yan F, Zhang C, Zheng Y, et al. The effect of poloxamer 188 on nanoparticle morphology, size, cancer cell uptake, and cytotoxicity. *Nanomedicine*. 2010;6(1):170–178.
47. Gelperina S, Kisich K, Iseman MD, Heifets L. The potential advantages of nanoparticle drug delivery systems in chemotherapy of tuberculosis. *Am J Respir Crit Care Med*. 2005;172(12):1487–1490.
48. Hu CM, Zhang L. Therapeutic nanoparticles to combat cancer drug resistance. *Curr Drug Metab*. 2009;10(8):836–841.
49. Zhu H, Chen H, Zeng X, et al. Co-delivery of chemotherapeutic drugs with vitamin E TPGS by porous PLGA nanoparticles for enhanced chemotherapy against multi-drug resistance. *Biomaterials*. 2014;35(7):2391–2400.

50. Cheng D, Cao N, Chen J, Yu X, Shuai X. Multifunctional nanocarrier mediated co-delivery of doxorubicin and siRNA for synergistic enhancement of glioma apoptosis in rat. *Biomaterials*. 2012;33(4):1170–1179.
51. Wang H, Zhao Y, Wu Y, et al. Enhanced anti-tumor efficacy by co-delivery of doxorubicin and paclitaxel with amphiphilic methoxy PEG-PLGA copolymer nanoparticles. *Biomaterials*. 2011;32(32):8281–8290.
52. Hu CM, Aryal S, Zhang L. Nanoparticle-assisted combination therapies for effective cancer treatment. *Ther Deliv*. 2010;1(2):323–334.
53. Creixell M, Peppas NA. Co-delivery of siRNA and therapeutic agents using nanocarriers to overcome cancer resistance. *Nano Today*. 2012;7(4):367–379.
54. Deng X, Cao M, Zhang J, et al. Hyaluronic acid-chitosan nanoparticles for co-delivery of MiR-34a and doxorubicin in therapy against triple negative breast cancer. *Biomaterials*. 2014;35(14):4333–4344.
55. Sheng Y, Liu C, Yuan Y, et al. Long-circulating polymeric nanoparticles bearing a combinatorial coating of PEG and water-soluble chitosan. *Biomaterials*. 2009;30(12):2340–2348.
56. Yokoyama M, Okano T, Sakurai Y, Ekimoto H, Shibazaki C, Kataoka K. Toxicity and antitumor activity against solid tumors of micelle-forming polymeric anticancer drug and its extremely long circulation in blood. *Cancer Res*. 1991;51(12):3229–3236.
57. Abouzeid AH, Patel NR, Torchilin VP. Polyethylene glycol-phosphatidylethanolamine (PEG-PE)/vitamin E micelles for co-delivery of paclitaxel and curcumin to overcome multi-drug resistance in ovarian cancer. *Int J Pharm*. 2014;464(1–2):178–184.
58. Carlson LJ, Cote B, Alani AW, Rao DA. Polymeric micellar co-delivery of resveratrol and curcumin to mitigate in vitro doxorubicin-induced cardiotoxicity. *J Pharm Sci*. 2014;103(8):2315–2322.
59. Pei Y, Wu B, Cao Q, Wu L, Yang G. Hydrogen sulfide mediates the anti-survival effect of sulforaphane on human prostate cancer cells. *Toxicol Appl Pharmacol*. 2011;257(3):420–428.
60. Trachootham D, Lu W, Ogasawara MA, Nilsa RD, Huang P. Redox regulation of cell survival. *Antioxid Redox Signal*. 2008;10(8):1343–1374.
61. Attene-Ramos MS, Wagner ED, Gaskins HR, Plewa MJ. Hydrogen sulfide induces direct radical-associated DNA damage. *Mol Cancer Res*. 2007;5(5):455–459.
62. Stasko A, Brezova V, Zalibera M, Biskupic S, Ondrias K. Electron transfer: a primary step in the reactions of sodium hydrosulphide, an H2S/HS(-) donor. *Free Radic Res*. 2009;43(6):581–593.
63. Attene-Ramos MS, Wagner ED, Plewa MJ, Gaskins HR. Evidence that hydrogen sulfide is a genotoxic agent. *Mol Cancer Res*. 2006;4(1):9–14.
64. Predmore BL, Lefer DJ, Gojon G. Hydrogen sulfide in biochemistry and medicine. *Antioxid Redox Signal*. 2012;17(1):119–140.